Ecotoxicology and Environmental Safety 263 (2023) 115222

Contents lists available at ScienceDirect

Ecotoxicology and Environmental Safety

journal homepage: www.elsevier.com/locate/ecoenv

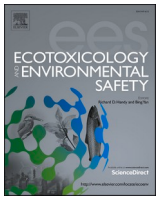

New insights into bacterial Zn homeostasis and molecular architecture of the metal resistome in soil polluted with nano zinc oxide

Dinesh Raghavan [a], Sreena Chuvatte Patinharekkara [a], Sheeja Thotten Elampilay [a,*], Vijesh Kumar Illathidath Payatatti [a], Sona Charles [a], Srinivasan Veeraraghavan [a], Jayarajan Kadiyalath [a], Sajith Vandana [b], Subila Kizhakke Purayil [a], Haritha Prasadam [a], Shalini Jayaraj Anitha [a]

[a] ICAR–Indian Institute of Spices Research, Marikunnu PO, Kozhikode, Kerala, India
[b] National Institute of Technology, NIT Campus PO, Kozhikode, Kerala, India

ARTICLE INFO

Keywords:
Predictive metagenomics
Soil bacterial communities
Soil pollution
Zn efflux
Zn homeostatic genes
Zn influx

ABSTRACT

Accumulation of nano ZnO (nZnO) in soils could be toxic to bacterial communities through disruption of Zn homeostasis. Under such conditions, bacterial communities strive to maintain cellular Zn levels by accentuation of appropriate cellular machinery. In this study, soil was exposed to a gradient (50–1000 mg Zn kg^{-1}) of nZnO for evaluating their effects on genes involved in Zn homeostasis (ZHG). The responses were compared with similar levels of its bulk counterpart (bZnO). It was observed that ZnO (as nZnO or bZnO) induced a plethora of influx and efflux transporters as well as metallothioneins (MTs) and metallochaperones mediated by an array of Zn sensitive regulatory proteins. Major influx system identified was the ZnuABC transporter, while important efflux transporters identified were CzcCBA, ZntA, YiiP and the major regulator was Zur. The response of communities was dose- dependent at lower concentrations (<500 mg Zn kg^{-1} as nZnO or bZnO). However, at 1000 mg Zn kg^{-1}, a size-dependent threshold of gene/gene family abundances was evident. Under nZnO, a poor adaptation to toxicity induced anaerobic conditions due to deployment of major influx and secondary detoxifying systems as well as poor chelation of free Zn ions was evident. Moreover, Zn homeostasis related link with biofilm formation and virulence were accentuated under nZnO than bZnO. While these findings were verified by PCoA and Procrustes analysis, Network analysis and taxa *vs* ZHG associations also substantiated that a stronger Zn shunting mechanism was induced under nZnO due to higher toxicity. Molecular crosstalks with systems governing Cu and Fe homeostasis were also evident. Expression analysis of important resistance genes by qRT-PCR showed good alignment with the predictive metagenome data, thereby validating our findings. From the study it was evident that the induction of detoxifying and resistant genes was greatly lowered under nZnO, which markedly hampered Zn homeostasis among the soil bacterial communities.

1. Introduction

Among the engineered nanoparticles (ENPs), nano ZnO (nZnO) is the third most commonly used NP (Peng et al., 2017) due to its high biocompatibility, physical and chemical stabilities and low cost. Estimates of nZnO concentration were found to range from 3.1 to 31.0 μg kg^{-1} in soil and between 76.0 and 760.0 μg L^{-1} in water (Ghosh et al., 2016). However, considering its unflagging production and consumption, its accumulation in the environment is bound to increase multi-fold (Shen et al., 2015), mainly due to reckless and unsafe disposal into soil. It is common knowledge that nZnO is very toxic, since it can dissolve rapidly and release Zn ions either singly or in combination with the remaining nZnO (Aruoja et al., 2009; Eixenberger et al., 2017). In natural environments like the soil, nZnO will be firmly sorbed on soil colloids and, therefore, exhibit lowered mobility (Zhao et al., 2012). Such accumulation could be harmful to microbial communities thereby hampering key soil nutrient cycles and processes. The toxicity mechanisms include cell surface alterations, penetration into the cytoplasm,

Abbreviations: bZnO, bulk zinc oxide; CDF, cation-diffusion facilitator; ENPs, engineered nanoparticles; HM, heavy metal; MRGs, metalloregulatory genes; MTs, metallothioneins; NP, nanoparticle; nZnO, nano zinc oxide; RND, Resistance-Nodulation-Division; TBDR, TonB-dependent receptor; ZHGs, zinc homeostatic genes.

* Correspondence to: ICAR-Indian Institute of Spices Research, Marikunnu PO, Kozhikode, Kerala 673012, India.
E-mail address: tesheeja@gmail.com (S.T. Elampilay).

https://doi.org/10.1016/j.ecoenv.2023.115222
Received 27 March 2023; Received in revised form 19 June 2023; Accepted 29 June 2023
Available online 6 July 2023

excessive production of reactive oxygen species, severe membrane aberrations, endoplasmic reticulum stress, DNA damage, protein oxidation, disarray in energy transduction, discharge of toxic elements and ultimately cell death (Singh et al., 2020).

Though Zn is crucial for essential functions in bacterial cells like DNA synthesis, transcription and translation, stabilizing diverse Zn-finger proteins and as cofactor for numerous metalloenzymes, its excess is toxic (Blencowe and Morby, 2003). Hence, maintenance of optimum intra-cellular Zn concentration is imperative for the survival of bacterial communities. So, the dilemma that bacterial cells face is 'homeostasis' *i.e.* bring in sufficient Zn using membrane uptake (influx) pumps while simultaneously regulating the membrane efflux pumps for flushing out excess Zn (Ducret et al., 2022). This homeostasis is regulated by mechanisms involving intra-cellular Zn buffering and sensing by transcription factors involved in either Zn influx/uptake or efflux/intra-cellular sequestration (Mikhaylina et al., 2018). High Zn in the environment promotes selection of resistant microbes harboring either chromosomal or plasmid level genes for maintaining Zn homeostasis within the cell (Blencowe and Morby, 2003). The different adaptation strategies imperative for survival of microbes under Zn stress include reducing the sensitivity through permeability barriers, enhancing efflux by transporters, enzymatic detoxification, reduction of metal ions and extracellular and intracellular sequestration (Blencowe and Morby, 2003; Blindauer, 2015). Our earlier studies on and predictive metagenome approach (Dinesh et al., 2023a, 2023b) have provided unprecedented insights into the genetic potentials of bacteria for a comprehensive view of the Zn resistome. Though next generation sequencing (NGS) has been extensively used to study nZnO toxicity in varied environments including soil (Shen et al., 2021; Meli et al., 2016), studies on its effects on an array of influx, efflux and metalloregulatory genes (MRGs) controlling abundance of metal trafficking proteins and membrane transporters combinedly regulating Zn homeostasis in soil bacterial communities are absent.

The presence of highly efficient heavy metal (HM) uptake/transport/efflux/detoxification systems operating within bacteria is predicted for bioremediation of HM polluted soils (Salam et al., 2020). Thus, HM resistance mechanism of adapted communities in contaminated environment is required to develop bioremediation strategies. Zinc homeostasis has been studied in pure cultures of several bacteria like *Bacillus subtilis* (Moore and Helmann, 2005), *Salmonella enterica* (Ammendola et al., 2007), *Pseudomonas aeruginosa* (Ducret et al., 2021; Pederick et al., 2015), *Bacillus anthracis* (Kandari et al., 2019) and *Escherichia coli* (Xu et al., 2019). However, the soil microbial ecosystems are often complex with many uncultivated bacteria and the resistance systems seen in cultivated strains are vastly different from complex communities. The most widespread system such as soil is, therefore, important, particularly in ecotoxicological studies, where metal resistant genes are used as bioindicators of metal pollution (Gillan, 2016). Also, the linkage between the dominant bacterial taxa and the functions is poorly understood, which is a major drawback in designing effective management and bioremediation strategies for nZnO polluted soils.

Hence, we aimed at understanding the overall Zn homeostasis and detoxification mechanisms among bacterial communities in soil polluted with nZnO and attempted to explore the Zn transporter families to verify their roles in relieving nZnO toxicity through mechanisms such as intracellular or extracellular precipitation, active efflux and transformation to lesser toxic species. Attempts were directed to comprehend the nature of co-occurrence and correlation patterns within and between soil bacterial communities and ZHGs, identification of possible hosts of these genes and elucidating gene-regulatory and other complex networks. For this purpose, we used soils spiked with nZnO representing both low and medium Zn levels (50, 200 mg kg^{-1}) and higher levels of 500 and 1000 mg Zn kg^{-1} relevant to ecotoxicological studies. The nZnO treated soils were compared with those treated with bulk ZnO (bZnO) because reports indicated that the latter causes toxicity similar to nZnO in bacteria (Heinlaan et al., 2008). We hypothesized that as Zn deficiency disrupts normal biological functions and excess induces cytotoxicity, a large collection of ZHGs would be triggered (Xia et al., 2021), with differential responses under nZnO and bZnO. It was also hypothesized that these Zn resistance systems may further impact homeostasis of other heavy metals like Cu and Fe in soils (Nies, 2003). The present study explores, for the first time, the interrelationships between community structure and ZHGs encompassing influx and efflux proteins and regulatory transcription factors in soils exposed to nZnO and provides new insights into the detailed mechanism adopted by the bacterial communities exposed to Zn toxicity. Understanding the selective pressure exerted by nZnO on bacterial communities and the corresponding resistance mechanisms could divulge their biogeochemical consequences and applications.

2. Materials and methods

2.1. Sample collection, illumina sequencing and mining of ZHGs

Soil microcosm setup, metagenomic sequencing and tools, softwares and databases for OTU taxonomies and functional profiles are as per Dinesh et al. (2023a). Briefly, soil (sandy clay loam, pH-7.21, available Zn content- 1.26 mg kg^{-1}) pre-incubated for 7 days at 28 $\pm$ 2^0 C was placed in microcosm (100 g, dry-weight equivalent,) and spiked with different levels of Zn (0, 50, 200, 500 and 1000 mg kg^{-1}) as nZnO (Sigma Aldrich, <50 nm) or bZnO (Sigma Aldrich). The experiment had three replications and the ZnO sources were mixed with the soil using the dry spiking method of Hund-Rinke et al. (2012). The microcosms were maintained at 60.0% WHC in a temperature-controlled glass house (28 $\pm$ 2^0 C) and soil samples were drawn on the 60th day. Soil available Zn at the end of the experiment was extracted using DTPA reagent (Lindsay and Norvell, 1978) followed by estimation of Zn using an atomic absorption spectrophotometer (Varian AA240FS). DNA samples from soil microcosm were subjected to amplicon sequencing (Illumina MiSeq v.2.4.60.8). Prediction of functional profiles was performed with Tax4Fun using OTU Table of taxonomic data as per Silva's database (Dinesh et al., 2023a). Marker KEGG orthologs (KOs) for Zn homeostasis mechanisms and their regulators were retrieved (Blindauer, 2015; Suryawati, 2018; Capdevila et al., 2016) and cross verified using KEGG database. The details of ZHGs are available at http://14.139.189.30/eznprobe/.

2.2. qRT-PCR validation of predicted metagenome data

Soil RNA was isolated using RNeasy Power Soil Total RNA kit (Qiagen, Germany) and quantified using spectrophotometer (Denovix, USA). cDNA synthesis was done from 250 ng of RNA using Revertaid cDNA synthesis kit (Thermofischer, Lithuania) and used for PCR experiments. The expression of major efflux genes *viz., CzcA* (Nongkhlaw and Joshi, 2019), *ZntA,* and minor system *viz.*, *YiiP* (Ouyang et al., 2022), at 1000 mg Zn kg^{-1} of ZnO was evaluated in Rotor Gene Q (Qiagen, Germany) using Quantinova SYBR Green PCR kit (Qiagen, Germany). Cycling parameters were 95 °C for 5 min followed by 40 cycles of 94 °C/30 s and 60 °C/30 s using16S rRNA internal standard.

2.3. Statistical analysis

The differences in abundance of most dominant taxa at the phylum and genus level in treatments were visualized using bar graph. The relative abundance (RA) of each gene in total community was calculated by comparing the sequence number of specific genes with total sequence number of selected samples. The changes in RA in treatments are represented as percent increase or decrease compared to control. Clustered heatmap of abundance of ZHGs was built for establishing relationships with Zn treatments and RA of KEGG orthologs. Principal Coordinate Analysis (PCoA) plots based on weighted Unifrac distances were calculated for biologically meaningful patterns of ZHG distribution. The

associations between the ZHGs and dominant taxa in treatments were analyzed using the Procrustes test. A function-taxa bipartite network was constructed from significant ($R \geq \pm 0.50$; $P < 0.05$) function-taxa relationships using Cytoscape v. 3.1.1 (Shannon et al., 2003). The topological parameters in Cytoscape were calculated using the tool network analyser (Assenov et al., 2008). Statistical analyses and data visualizations were performed using R software v.4.2.2.

3. Results

3.1. Bacterial community structure

We were able to detect 34 phyla, of which 12 showed RA> 1.0%. Higher the Zn, the more significant ($P < 0.05$) were the variations in community composition (Fig. S1a and b). Important phyla like Proteobacteria, Firmicutes, Actinobacteria, Planctomycetes, Acidobacteria, Chloroflexi and Bacteroidetes accounted for > 80.0% of dominant phyla. Proteobacteria increased in RA with Zn levels as nZnO (21.4–26.6%). Under Proteobacteria, the genus *Sphingomonas* showed a marked increase in RA with increasing Zn levels, with maximum at 1000 mg Zn kg^{-1} as nZnO (106.2%) while the genus *Microvirga* showed a reduction, with lowest RA at 1000 mg Zn kg^{-1} as nZnO. Firmicutes decreased in RA with increasing Zn levels as nZnO (15.4–11.7%). The main genera under this phylum *viz.*, *Bacillus* registered maximum decrease at 1000 mg Zn kg^{-1} as bZnO (23.7%). Actinobacteria constituting genera *Rubrobacter*, *Nocardioides* and *Streptomyces* exhibited varying degrees of decrease in RA due to Zn addition as nZnO or bZnO. The RA of dominant genera under Acidobacteria *viz.*, *Bryobacter, Candidatus Solibacter* and *RB41* was found to decrease in all nZnO treatments compared to bZnO). The results, therefore, suggested that Proteobacteria, Planctomycetes, Acidobacteria, and Bacteroidetes were the major phyla that increased with Zn addition irrespective of ZnO size.

3.2. Zinc resistome and associated functions

Bacteria under metal pollution develop resistance mechanisms that enable efficient detoxification and transformation of toxic forms to non-toxic forms. The most important resistance functions involve a) membrane transport b) influx c) efflux d) intracellular sequestration and trafficking by metallothioneins (MTs) and metallochaperones. About 40 genetic determinants and their regulators that mediate Zn homeostasis were discerned in the study (Table S1; Fig. 1).

3.2.1. Membrane-bound transport system

High soil Zn (mean 1248.00 ± 38.57 mg kg^{-1} and 1038.67 ± 18.77 mg kg^{-1} in case of 1000 mg Zn kg^{-1} as nZnO and bZnO, respectively) (Table S2), favored passive transport more than energy dependent system as evident from over representation of porin genes. *OmpW* showed increased abundance at 500 mg Zn kg^{-1} as nZnO (28.4%) and 1000 mg Zn kg^{-1} as bZnO (30.3%). In case of *OmpF*, *OmpC* and *OmpE/PhoE,* increased RA was observed at 200 mg Zn kg^{-1} as nZnO (91.3%, 64.9% and 171.2% respectively), while under bZnO the maximum abundance of the genes were 46.9% at 1000 mg Zn kg^{-1}, 10.6% at 50 mg Zn kg^{-1} and 65.2% at 500 mg Zn kg^{-1} respectively.

Besides OMPs, the genes encoding the second category of integral membrane protein TonB-dependent receptor (TBDR), *ZnuD* enhanced in treatments with maximum at 500 mg Zn kg^{-1} as nZnO (29.2%) and 1000 mg Zn kg^{-1} as bZnO (27.6%). TonB-ExbB-ExbD energy transduction system that energizes ZnuD was also identified in the study. The abundance of *TonB* was found to decrease with Zn addition with maximum decrease at 500 mg Zn kg^{-1} as nZnO and bZnO (7.1% and 6.8%, respectively), while it was enhanced in the control treatment. In

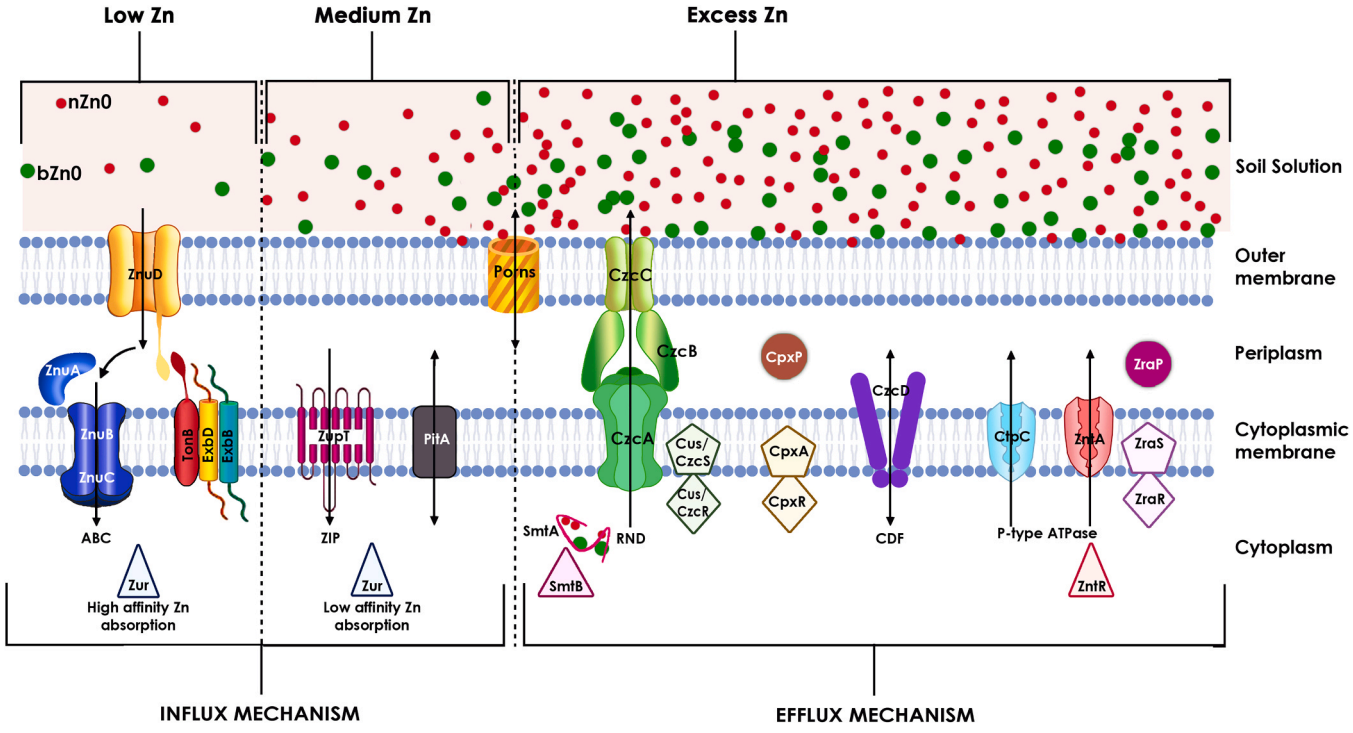

Fig. 1. An overview of the important Zn homeostatic genes identified in the bacterial metagenome in soils spiked with nZnO and bZnO, exemplified for Gram-negative bacteria. Included are the representative orthologs under the following categories:.
A. Influx- a. Constitutively expressed outer membrane porins involved in passive Zn transport under excess Zn b. High-affinity importers such as ABC transporters (ZnuABC), TBDR (ZnuD, TonB-ExbB-ExbD) under Zn deficiency c. Low-affinity importers such as PitA, ZupT under medium Zn B. Efflux- a. P-type ATPase (CtpC and ZntA), b. CDF-type (CzcD/ZitB) c. RND-type (CzcCBA) under excess Zn. C. Metalloregulators- a. Metallothionein SmtA, b. Metallochaperones ZraP and CpxP under Zn excess. D. Regulators- Zur, ZntR, Cus/CzcSR, SmtB, ZraSR, CpxAR are also indicated. Relevant details of ZHGs and their orthologs/homologs identified in the study are available in Table S1.

contrast, the RA of *ExbB/ExbD* was found to increase at 1000 mg Zn kg^{-1} as nZnO (28.5%) and bZnO (23.1%).

3.2.2. Zinc influx systems

The high affinity uptake systems identified were ATP binding cassette (ABC) system, consisting of (i) ZnuABC (Zn), (ii) TroABC (Mn/Zn/Fe), (iii) ABC.ZM.SPA (Zn/Mn) and (iv) SitABCD (Mn/Fe). Decrease in RA at higher levels of nZnO and bZnO was observed except for *SitABCD*. Lower ($P < 0.05$) RA of *ZnuABC* and *TroABC* was observed at 1000 mg Zn kg^{-1} as bZnO (7.5% and 17.1%, respectively) as compared to nZnO. For *ABC.ZM.SPA*, the decrease was marginally lower under bZnO (12.5%, at 1000 mg Zn kg^{-1}) compared to nZnO (13.6%, 500 mg Zn kg^{-1}). However, in case of *SitABCD*, the RA was high in Zn treatments, with highest at 200 mg Zn kg^{-1} as nZnO (46.8%).

The genes for other high affinity transporters *viz., ZntB* (*CorA/MIT*) and *YbtX* registered significantly higher ($P < 0.05$) RA in ZnO. *ZntB* levels were higher ($P < 0.05$) at 200 mg Zn kg^{-1} as nZnO (43.9%) and lower under bZnO with maximum of 37.3% at 500 mg Zn kg^{-1}. *YbtX* indicated similar trend with significantly higher ($P < 0.05$) abundance under nZnO (38.6% at 200 mg Zn kg^{-1}) compared to bZnO (30.2% at 500 mg Zn kg^{-1}). The main *ZIP* transporter identified was *ZupT*. The RA of *ZupT* was higher ($P < 0.05$) in control and lowest at 1000 mg Zn kg^{-1} as bZnO (23.2%) and nZnO (7.5%), indicating a subdued response under bZnO. In contrast, *PitA* was enhanced under nZnO (32.3%) and bZnO (17.4%) at 500 mg Zn kg^{-1}. Important influx regulator Zur, that binds to *ZnuA* promoter and repress *ZnuABC* under Zn sufficiency could also be identified, while *YbtA* the regulator of *YbtX* increased in Zn treatments as nZnO or bZnO.

3.2.3. Zinc efflux systems

3.2.3.1. P-type ATPases. *ZntA*, encoding a P-type ATPase that transports Zn across cytoplasmic membrane showed significant ($P < 0.05$) abundance at 500 mg Zn kg^{-1} (3.9%) as bZnO compared to corresponding level of nZnO (0.14%). *CtpC*, coding for another P-type ATPase decreased ($P < 0.05$) under nZnO (30.8% at 1000 mg Zn kg^{-1}), though under bZnO an increase in RA was observed (4.7% at 200 mg Zn kg^{-1}).

3.2.3.2. Cation-diffusion facilitator (CDF) proteins. *CzcD/ZitB*, showed no significant dose or size-dependent variation, with slight enhancement under bZnO (0.66% at 1000 mg Zn kg^{-1} as bZnO and 0.4% at 50 mg Zn kg^{-1} as nZnO). *YiiP* (*FieF*), increased with Zn addition, with greater ($P < 0.05$) abundance at 500 mg Zn kg^{-1} as bZnO and 200 mg Zn kg^{-1} as nZnO (21.1%).

3.2.3.3. Resistance-Nodulation-Division (RND) efflux proteins. The RND family proteins that span the inner and the outer membrane and transport cations from the periplasm across the plasma membrane encoded by *CzcCBA* and *CusFCBA* operon showed greater RA under high Zn, especially at 1000 mg Zn kg^{-1} as bZnO (24.6% and 24.9%, respectively). Under nZnO, maximum RA was registered at 500 mg Zn kg^{-1} (21.9% and 13.5%, respectively). The efflux genes identified in the study were regulated by ZntR and Cus/CzcSR TCS, which increased in treatments and a partial regulator CzcD/ZitB, which is a cation efflux system regulating CzcCBA.

3.2.4. Sequestration and trafficking of Zn

3.2.4.1. Molecular metallothioneins and chaperones. Physical sequestration of metal by binding proteins to prevent its damage from metal sensitive targets is a mechanism of heavy metal resistance involving several metallothioneins and chaperones. SmtA, the first reported bacterial heavy metal binding metallothionein was enhanced in high Zn spiked soils, with significant ($P < 0.05$) increase at 500 mg Zn kg^{-1} as nZnO (28.6%) followed by bZnO at similar level (22.3%). Zinc bound metallochaperone ZraP showed higher RA in Zn treatments with maximum increase under nZnO at 200 mg Zn kg^{-1} (22.7%). In contrast, the RA of *CpxP* was enhanced in the control treatment and treatments with lower levels of nZnO (17.9% at 200 mg Zn kg^{-1}), while, significant ($P < 0.05$) attenuation was observed at 1000 mg Zn kg^{-1} as bZnO (12.8%).

The heatmap of ZHGs and regulators indicated a dose-dependent variation *i.e.* the lower Zn levels clustered together with control, while higher Zn levels formed a separate cluster, irrespective of ZnO size (Fig. 2a). This was supported by PCoA (Fig. 2b). However, size-dependent variation was prominent at 1000 mg Zn kg^{-1} (Fig. 2c). At this level, influx related genes (*OmpF, OmpC, OmpE/PhoE, ZnuABC*, *TroABC*, *ABC.ZM.SPA, SitABCD, ZntB, YbtX, PitA, ZupT*) were augmented under nZnO while the efflux genes *ZntA, CtpC, CzcD/ZitB*, *YiiP*, *CzcCBA* and *CusFCBA* were attenuated. However, under bZnO this was reversed. In the control treatment, Zn limitation was evident from the over-representation of influx genes and attenuation of efflux genes (Fig. 2c). The presence of several ribosomal proteins, with 17 being over-represented, also endorsed the Zn deficient condition in the control treatment (Fig. S2).

3.3. Linking influx and efflux genes to bacterial taxa using a function-taxa bipartite network

Correlation between dominant bacterial taxa and ZHGs was evaluated by Procrustes analysis (Fig. S3). Under both nZnO and bZnO, strong correlations were observed between bacterial taxa and ZHGs. However, the correlations were greater under nZnO ($M^2 = 0.0697$, $r = 0.9645$, $P < 0.05$) than bZnO ($M^2 = 0.2197$, $r = 0.8833$, $P < 0.05$). Besides, a network analysis was performed to find the relationship between individual taxa and ZHGs. Topological properties of co-occurrence network indicated contrasting associations under nZnO and bZnO (Table S3). The network, comprising of 12 genera and 32 ZHGs, exhibited eight and six modules under nZnO and bZnO, respectively (Fig. 3). In case of nZnO, in module I, the genes linked to secondary homeostatic system mediating a small degree of Zn resistivity were driven by *Bacillus* (Firmicutes), *Rubrobacter* and *Nocardioides* (Actinobacteria), while in module II, the genes primarily involved in Zn homeostasis were driven by *Sphingomonas* (Proteobacteria) and *Nitrospira* (Nitrospirae). The genera in other modules were found to be associated with secondary homeostatic systems. However, under bZnO the associations were different. In module I, *Bacillus* (Firmicutes), *Rubrobacter*, *Nocardioides* (Actinobacteria) and *Microvirga* (Proteobacteria) were linked to the main influx and efflux systems and in module II, the genes linked to secondary homeostatic systems were associated with *Sphingomonas* (Proteobacteria) and *Flavisolibacter* (Bacteroidetes). *Streptomyces* (Actinobacteria) was found to be linked with *ZntA* under both nZnO and bZnO. The genera with the greatest number of connections with ZHGs (hub) were *Bacillus* and *Sphingomonas* in module I and II respectively under nZnO, while it was *Rubrobacter* and *Sphingomonas* under bZnO.

Based on the number of connections between taxa and genes, it could be deduced that the contribution of major uptake system (ZnuABC) was high (79.2%) under nZnO, compared to bZnO (63.2%), while that of minor system (ZupT) was high under bZnO (36.8%) compared to nZnO (25%) Among the efflux genes, the high resistance systems *viz.*, CzcCBA, ZntA and CtpC contributed 73.0% under nZnO compared to bZnO (82.0%), while the contribution of minor systems *viz.*, CzcD/ZitB and YiiP was high under nZnO (30.0%) than bZnO (18.0%).

3.4. qRT-PCR validation of predicted metagenome data

Validation of predicted metagenome data was done by expression profiling of important efflux/resistance genes *CzcA, ZntA* and *YiiP*. Upregulation was observed with 4.4-fold increase of *CzcA* under nZnO and 7-fold increase under bZnO in comparison with control treatment. In case of *ZntA*, the expression was downregulated under nZnO (0.84

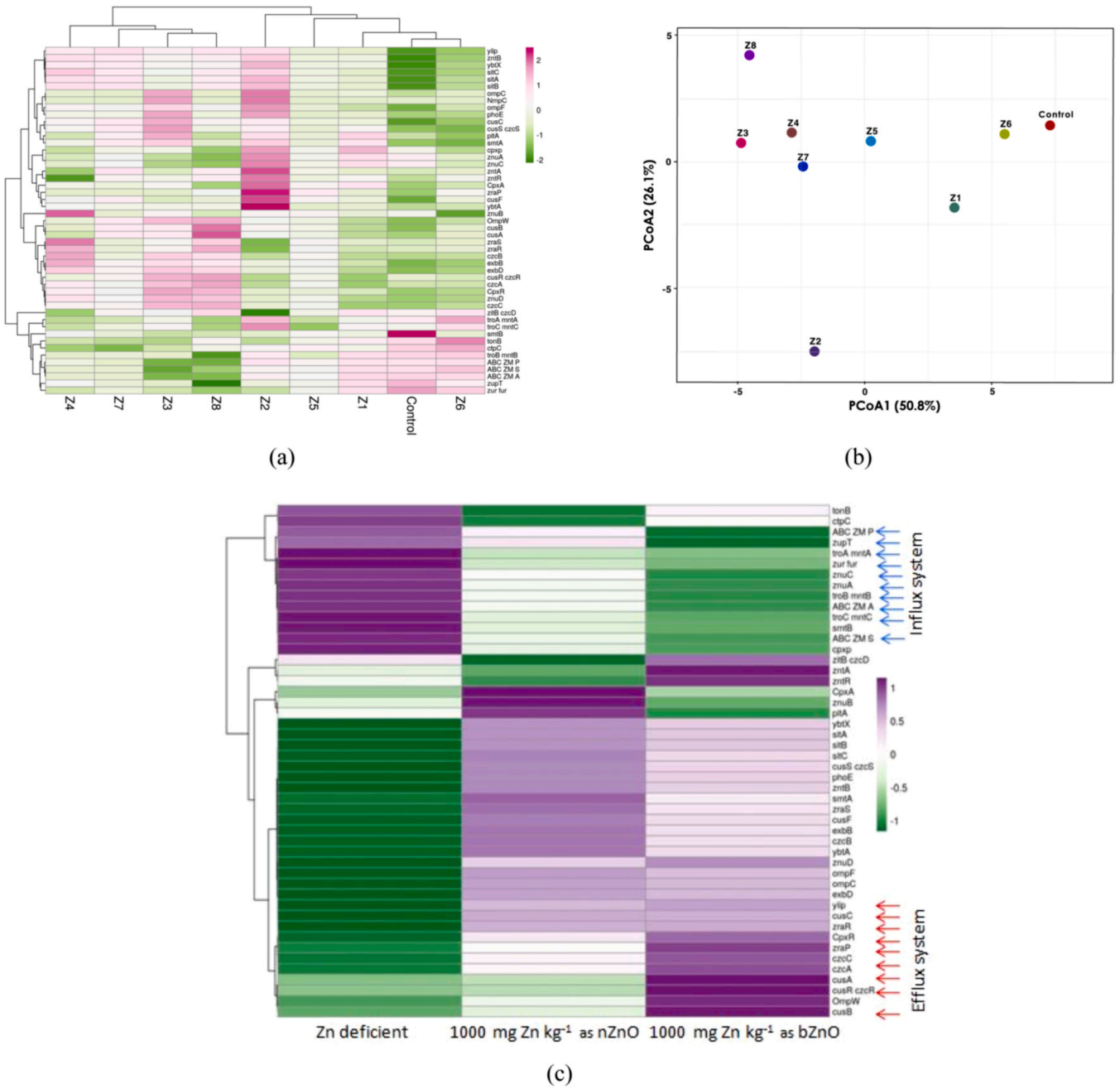

Fig. 2. Heat map of (a) dominant ZHGs and their regulators in the soil bacterial metagenome exposed to different levels of Zn as nZnO and bZnO [Control (No Zn), Z1- 50; Z2- 200; Z3–500; Z4–1000 mg Zn kg^{-1} as nZnO; Z5–50, Z6–200, Z7–500, Z8–1000 mg Zn kg^{-1} as bZnO] (b) Principal Coordinate Analysis (PCoA) based on weighted Unifrac distance matrices of ZHGs (c) dominant ZHGs and their regulators in control (Zn deficient) and soils spiked with 1000 mg Zn kg^{-1} as nZnO and bZnO.

fold) and upregulated under bZnO (1.67 fold) with respect to control treatment. The secondary efflux gene *YiiP* was upregulated in both, with greater impact under bZnO (2.83) compared to nZnO (1.67) (Fig. 4).

4. Discussion

Though Zn is essential to regulate numerous structural, regulatory and catalytic functions in bacteria, elevated levels can deplete protein thiols or competitively mismetallate binding sites of other metal ions, consequently impeding various physiological functions (Chandrangsu and Helmann, 2016; Xu et al., 2019). For survival it is imperative that the bacterial intracellular free Zn is maintained at extremely low levels *i.e.* from femto to pico molar levels (Blindauer, 2015). Zinc has been reported to function as a selective regulator of diversity and abundance as evidenced by decreased abundance of sensitive bacterial population and enhanced abundance of tolerant ones (Dinesh et al., 2023a, 2023b; Chen et al., 2021). The addition of Zn to agricultural soils activates Zn resistance systems used for uptake, transport, efflux and detoxification (Nies, 2003) mediated through certain genetically encoded survival systems encompassing Zn homeostasis (Capdevila et al., 2016). Studies on Zn homeostasis in Zn polluted scenarios were predominantly centered on isolated strains (Moore and Helmann, 2005; Ammendola et al., 2007; Pederick et al., 2015; Xu et al., 2019; Ducret et al., 2021; Kandari et al., 2019) and in case of natural environments emphasis has been on co-selection of antibiotic resistance genes (Shen et al., 2021). Apparently, Zn coping mechanisms and functional consequences are not

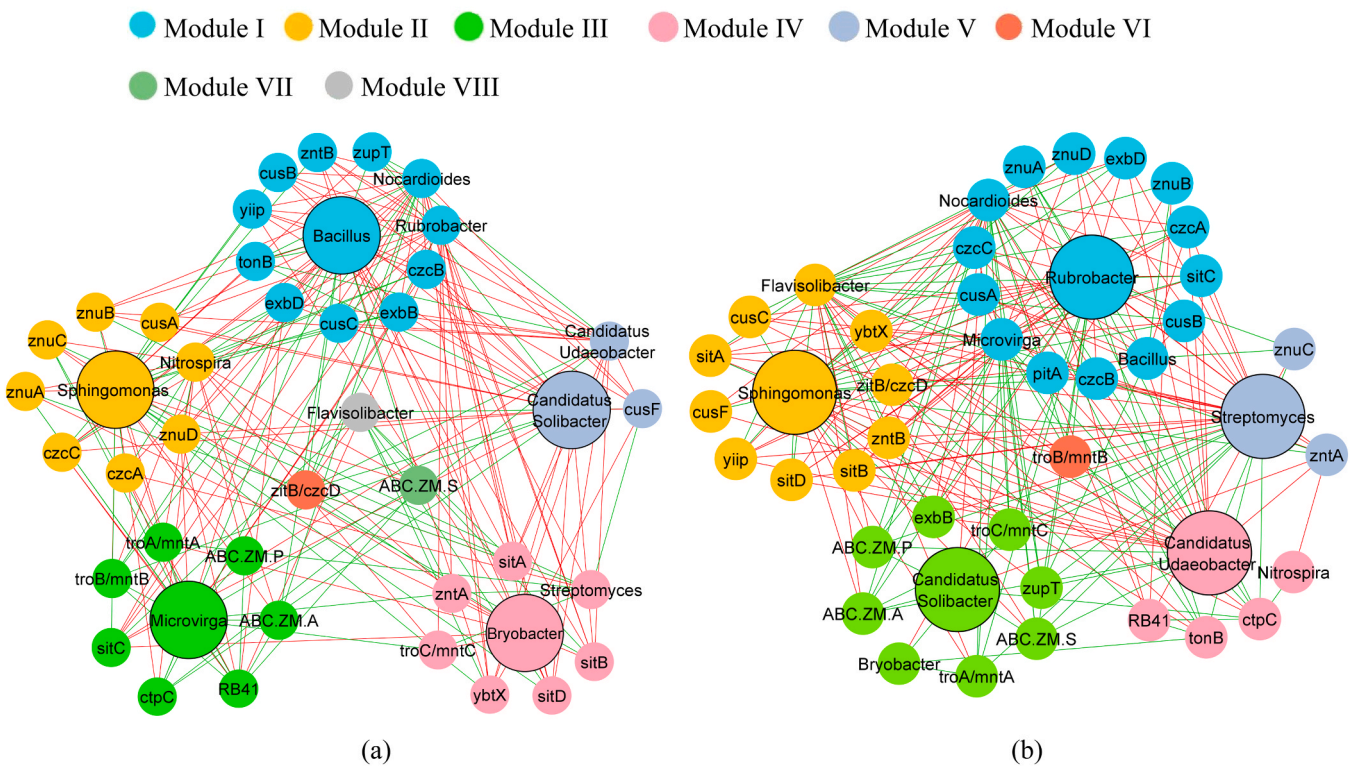

Fig. 3. Co-occurrence network indicating the interaction between Zn homeostatic genes and dominant bacterial genera in soils spiked with (a) nZnO and (b) bZnO. Lines connecting two nodes represent a group of strong ($R > \pm 0.5$) and significant correlations ($P < 0.05$). Green lines indicate a positive correlation, while red lines indicate a negative correlation. Nodes are colored according to modularity classes. Hubs of modules are indicated in larger circles.

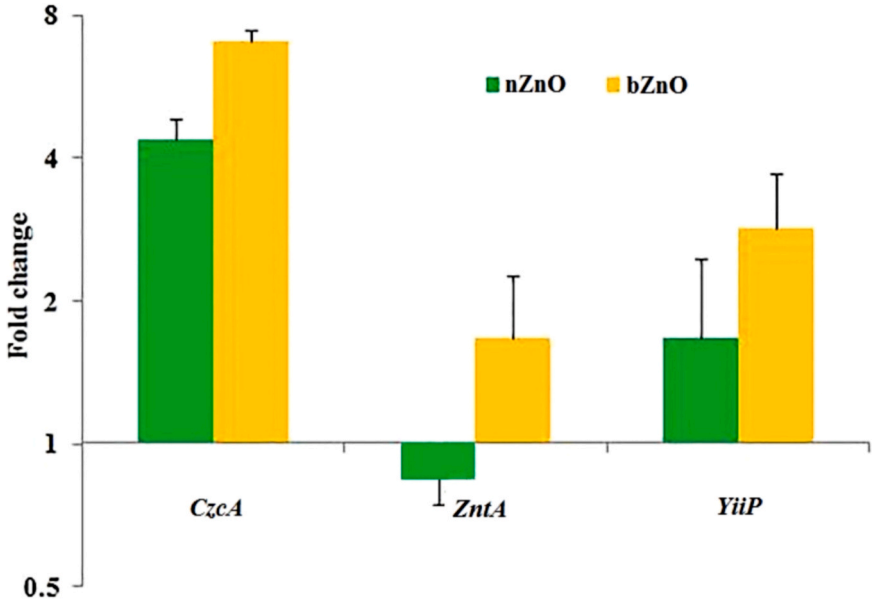

Fig. 4. Quantitative real-time PCR analysis indicating expression of efflux genes at 1000 mg Zn kg^{-1} as nZnO and bZnO (mean ± SE). The fold change of gene expression is measured relative to the control treatment (No Zn) (control=1, > 1.0 indicates up-regulation and < 1.0 indicates down-regulation.

well described in soil metagenomes. Also, no information is available on potential bioindicator strains for bioremediation of nZnO contaminated soils and bioindicator functions, which can be utilized as markers for easy and rapid detection of nZnO toxicity. Hence, we collated information from available literature to verify the metal sensing metalloregulatory proteins, transporters, chaperones, sensors and other small molecules involved in soil bacterial Zn homeostasis (Blindauer, 2015; Capdevila et al., 2016; Suryawati, 2018; Xia et al., 2021). A gradient of nZnO including ecotoxicologically relevant levels were compared along with the bulk counterpart (bZnO) for evaluating size effects. We employed predictive metagenomic profiling (PMP) as several studies have endorsed it as an economical and useful supplement to 16 S rRNA analyses in preparatory metagenome investigations (Jani et al., 2018; Auti et al., 2019; Dinesh et al., 2023a, 2023b).

4.1. Zinc homeostatic mechanisms

4.1.1. Low and high affinity Zn uptake systems

Functional characterization of inferred metagenomes indicated abundance of membrane bound porins, high affinity uptake transporters such as ZnuABC and low affinity systems such as ZupT guiding both passive as well as energy driven influx of Zn into bacterial cells (Ducret et al., 2021; Hantke, 2005; Ammendola et al., 2007) in the control treatment without added Zn. Among these, a constitutively expressed and diffusion gradient driven passive transport of Zn ions to periplasm, evident in many Gram-negative bacteria (Ducret et al., 2021) mediated *via* major porin genes like *OmpC, OmpF, OmpE/PhoE* was prominent. Under excess Zn, the abundance of these transporters was more under nZnO than bZnO indicating a more toxic environment under the former. Contrarily, an enhanced adaptation capability of bacteria to stress induced anaerobiosis mediated by over representation of *OmpW* (Xiao et al., 2016) was evident under bZnO. Endorsing this observation, global anaerobic transcriptional regulators of CFP/FNR family (nitrogen oxide reductase regulator) and ArcA, which carries OmpW in its regulon (Xiao et al., 2016) could be identified at higher levels of added Zn as nZnO or bZnO. This indicated a blockage in the aerobic metabolism and Fnr dependent activation of *ArcA* transcription for adaptation to anaerobic conditions under Zn excess (Compan and Touati, 1994). The proposed role of OmpW in carbon and energy metabolism during anaerobic adaptation indicated a probable shift from aerobic to anaerobic lifestyle of bacteria under Zn toxicity. Moreover, we have several reports that endorse induction of oxidative stress as a consequence of HM toxicity (Behera et al., 2014). These types of situations are much prevalent and studied and validated in many pure culture studies as well as natural and simulated anaerobic and aerobic experiments (Xiao et al., 2016), but is lacking under soil and other natural systems with HM toxicity.

The abundance of TonB dependent receptors (TBDRs) *viz.,* ZnuD and PA1922 driven by the TonB-ExbB-ExbD system indicated that the energy driven active acquisition of Zn involved integral membrane proteins for importing Zn ions from soil to periplasm and further to cytoplasm (Pederick et al., 2015; Bobrov et al., 2014). Enhanced abundance of *TonB* in control may be considered as a coping mechanism adopted by bacteria under Zn deficiency. Lower abundance of *ZnuD* in control further indicated that it is not involved in Zn transport under deficient conditions contrary to earlier observations. The presence of these transporters suggested that Zn is transported as Zn ions rather than in the chelated form through the membrane. Also, presence of these secondary systems in addition to the primary import system, ZnuABC indicated enhanced effort by soil bacterial communities towards maintaining homeostasis.

Under depletion, additional Zn uptake systems are induced to warrant cellular supply of Zn and in addition to the membrane mediated transport, high abundance of energy-driven high substrate specific systems and gradient driven non-specific systems (Wątły et al., 2016; Blindauer, 2015) were reflected. In the control treatment with low Zn (1.22 ± 0.09 mg Zn kg^{-1}; Table S2), the high affinity uptake systems primarily involved in import were the highly specific, Zn inducible ZnuABC system and all the components of this tripartite system including periplasmic Zn^{2+} (solute) binding protein, ZnuA, the inner membrane channel protein, ZnuB and the ATP enzyme protein, ZnuC, that provides energy for Zn^{2+} transport (Hantke, 2001; Xia et al., 2021) were identified. Over representation in the control treatment indicated de-repression of the operon during deficiency to increase Zn uptake, while decrease in abundance under excess Zn as both nZnO and bZnO indicated attenuation of these transporters to maintain intracellular Zn within safe limits (Xia et al., 2021). Interestingly, at 1000 mg Zn kg^{-1} as nZnO an enhancement of *ZnuB* and attenuation of *ZnuA* and *ZnuC*, suggested *ZnuB* mediated enhancement in biofilm functions and virulence, as a survival strategy under contaminated environments (Dinesh et al., 2023a). Reports by Xia et al. (2021) and Ammendola et al. (2007), regarding loss of virulence due to deletion of *ZnuABC* as well as its crucial role in biofilm formation and virulence under Zn deficiency also substantiated our observations. Increased abundance of *ZnuABC* under nZnO than bZnO implied that virulence functions are comparatively enhanced under the former (Gonzalez et al., 2019).

Detection of low affinity transporters like Zn ion regulatory protein ZIP (Zn-Fe permeases or ZRT/IRT-like protein) family indicated that Zn influx and intracellular redistribution also occurred under less extreme environments. However, functions and mechanism of action of ZIP transporters in homeostasis of bacteria is not yet well understood, except for a few based on genome sequences or transcriptomics (Sabri et al., 2009). Though *ZupT* is normally obscured by *ZnuABC*, higher abundance in control is indicative of its ability for constitutive expression even at low levels as an adaptive mechanism under Zn deficiency (Xia et al., 2021) as well as when primary uptake systems are dysfunctional (Grass et al., 2005). Our study also provided evidence for its involvement in Zn uptake under limitation, contrary to observations by Wątły et al. (2016) and Hantke (2005). *ZupT* also indicated a higher abundance under nZnO than bZnO leading to a greater influx and toxicity in the former. Low affinity, unspecific absorption systems that control Zn transport, catalyzing its rapid exchange *via* chemical osmotics (Hantke, 2001) were evident and identification of constitutively expressed, high rate, unspecific transporter PitA, indicated another entry route for Zn in its phosphate form (Beard et al., 2000). Colonization of such bacteria with enhanced *PitA* coupled with over representation under nZnO than bZnO indicated a relatively more toxic environment under the former. Interestingly, certain dual transporters involved in both influx (Gati et al., 2017) and efflux (Blindauer, 2015) *viz.,* ZntB of CorA family, dominated in ZnO treatments, despite it not having an apparent role in imparting metal resistance (Chaoprasid et al., 2015), substantiating its role as a class 2 porter (Blindauer, 2015). *YbtX*, coding for a dual transporter involved in uptake of both Zn and Fe was enhanced under both nZnO and bZnO indicating augmentation of primary import system (ZnuABC) for maintaining homeostasis (Bobrov et al., 2014). On the other hand, several large and small subunit ribosomal proteins and paralogs (Capdevila et al., 2016) identified in the control treatment indicated replacement of essential Zn dependent proteins with non-Zn requiring proteins as an adaptive strategy under Zn limitation (Fig. S2). However, chaperone (COG0523 subfamily) mediated mismetallation of obligatory proteins normally deployed for adaptation under HM limitation (Capdevila et al., 2016) was not observed in our study. Thus under Zn deficiency, enhanced intake mediated by ABC transporters and ZupT (Fig. 2c), deployment of non-Zn requiring ribosomal proteins (Fig. S2) and a subdued efflux were the strategies for survival (Fig. 2c).

4.1.2. Zinc resistance determinants and efflux transporters

In both nZnO and bZnO treatments, the Zn rich milieu facilitated entry of excessive Zn to bacterial cell by both passive and active influx. The communities adapted themselves through a dose- dependent variation in the abundance of genes and gene families, though the total number of functional genes within communities did not change with Zn gradient (Fig. 2a and b). The cellular detoxification and subcellular redistribution of Zn were predominantly dealt through primary and secondary Zn ion filter systems such as P-type ATPases, chemiosmotic cation diffusion facilitator (CDF) and resistance-nodulation-division (RND) pumps. Enhanced abundance of *ZntA* under both nZnO and bZnO indicated that P-type ATPase would be the primary efflux pump transporter under high soil Zn (Wang et al., 2012). However, at very high levels of 1000 mg Zn kg^{-1} as nZnO, a marked decrease indicated impairment of this export system at toxic levels. Lower abundance in control and enhancement under Zn excess indicated that it is not involved in import unlike other transporters repressed under Zn excess (Ducret et al., 2021). The higher abundance of the P type ATPase transporter CtpC under bZnO also indicated an effective export of Zn *via* this system as it is known to mediate survival by strong upregulation of up to 30 times on Zn exposure (Botella et al., 2011).

CDF category transporters such as CzcD (YbgR/ZitB) lacked a dose-/

size- dependent variation indicating their secondary role in imparting Zn resistance. YiiP (FieF) transporter that showed an increase in abundance under bZnO is implicated in multimetal transport and though it may not confer additional Zn resistance (Grass et al., 2001), it could play a protective role by virtue of its Zn binding sites (Lu and Fu, 2007). Hence, it could be presumed that CBA was the dominant transporter, which carried out outer membrane efflux either by removing periplasmic Zn transported there by ATPases or CDF transporters or by expelling Zn before they entered the cytoplasm. Additionally, the Zn transferred to the periplasm also played a major role in *CzcCBA* induction and active export of Zn (Nies, 2003).

Presence of tripartite efflux pumps of the RND family spanning inner and outer membranes indicated independent transport of Zn, which could have mediated Zn expulsion either by transition through the periplasm and expulsion *via* the trans envelope protein complex or by direct ejection from cytoplasm to extracellular medium without releasing to periplasm (Nies, 2003). The over representation of major structures *CzcCBA* under Zn excess, especially under higher levels of bZnO (Fig. 2c) indicated an exceptionally high resistance to Zn ions under bZnO, as the operon *czcCBA* is also flanked by a multitude of metal dependent regulatory genes (Nies, 2003).

4.1.3. Zinc chelation under Zn excess

Zinc sequestration mediated through bacterial metallothioneins such as SmtA, that is prominently induced by elevated Zn imparts enhanced capability to prevent deleterious interactions (Blindauer and Leszczyszyn, 2010). Over representation under nZnO indicated very high bioavailable Zn within bacterial cytoplasm than the cell associated concentration. While Zn binding is deployed to induce nutritional immunity and depletion to inhibit pathogen growth in host-mediated immune response, under soil ecosystems it is viewed as an adaptive strategy to shield bacteria from harmful effects of the metal ion. We also identified Zn bound metallochaperone ZraP that enhances tolerance by shielding Zn from intracellular environment preventing its interaction with cell components (Blencowe and Morby, 2003). The catalytic molecular chaperone activity of ZraP is Zn-dependent and over representation under 1000 mg Zn kg^{-1} as bZnO suggested enhanced Zn chelation and lowered Zn exposure to cell components (Petit-Härtlein et al., 2015). The abundance of *CpxP*, encoding a chaperone expressed in growth limited condition was found to be enhanced in the control treatment and lower Zn levels, while being attenuated at 1000 mg Zn kg^{-1} as bZnO indicating a reversal of function under Zn excess (Jubelin et al., 2005).

4.2. Function-taxa bipartite network analysis

A strong correlation between ZHG and dominant bacterial genera under nZnO in Procrustes analysis (Fig. S3) indicated a greater contribution of communities towards ZHG functions and a more disturbed environment. Network analysis also substantiated the above observation of differential adaptive strategies and bacterial associations under nZnO and bZnO (Fig. 3). While tolerant genera (increasing genera *viz., Sphingomonas and Nitrospira*) under nZnO deployed a shunting mechanism involving major influx (ZnuABC) and efflux (CzcCA) systems for detoxification, tolerant genera *Sphingomonas, Flavisolibacter* and *Bryobacter* under bZnO deployed minor uptake systems such as YbtX, ZntB, SitABCD, TroAC, ZupT, ABC.ZM.SPN, ExbB, which are mostly redundant, and were not observed to pair with efflux systems to form a regulated shunting mechanism for metal efflux. This indicated that the nZnO environment is relatively more toxic and requires an active shunting process to mediate homeostasis. Considering all the twelve dominant genera, greater number of connections with filter proteins like CzcD/ZitB and YiiP that are secondary to the main efflux system indicated a less effective Zn efflux under nZnO, while under bZnO the dominant genera were associated more with high resistance efflux systems. Therefore, it can be presumed that the core bacterial communities were able to better deploy a cohort of Zn efflux/detoxifying genes under bZnO than nZnO. The taxonomic affiliation of the resistance genes within a module in the network suggested co-occurrence of ZHGs and the bacterial genera under similar environmental pressure (Zhao et al., 2021). High positive correlations between *Sphingomonas* and ZHGs under both nZnO and bZnO indicated that it could be the major hosts of ZHGs (Fig. 3), substantiating their ability to survive in metal contaminated soils (Hu et al., 2021).

4.3. Interplay of Zn, Cu and Fe homeostatic pathways under excess Zn

Interestingly, the overrepresentation of influx transporters such as SitABCD, ZnuD and YbtX (Fe uptake) and CusFCAB (Cu efflux) in Zn treatments probably indicated perturbation of Fe and Cu homeostasis leading to an increased demand for Fe and decreased tolerance to Cu commonly observed in bacteria under Zn excess (Xu et al., 2019). Excess Zn could have induced Fe deficiency due to mismetallation enhancing the abundance of importers of Fe. Zn excess probably inflicted the primary Cu detoxification system *via* the Fe mediated indirect activation of secondary system, CusFCBA (Xu et al., 2019). Enhanced abundance of these transporters under nZnO suggested higher oxidative stress than under bZnO and an adaptive mechanism imparting resistance to oxidative stress through Fe acquisition (Sabri et al., 2008). This suggested that such stress adaptation processes may lead to widespread cross resistance, which might evolve as a serious environmental hazard.

4.4. Regulation of homeostasis under Zn excess

High adaptability of communities depicted by deployment of metalloregulatory genes and metallochaperones is supported by identification of numerous regulatory systems known to allow a rapid and targeted response to Zn availability. Identification of the most important regulators Zur (Fur family), ZntR (MerR family), SmtB (ArsR family), YbtA (AraC family) and TC regulatory systems (TCS) *viz.*, Cus/CzcSR, CpxAR (OmpR family), and ZraSR (NtrC family) suggested that the bacterial communities deployed an array of sensors and transcriptional regulators for retaining concentration of free and labile Zn in cytoplasm at an extraordinarily low level (femtomolar range) (Pederick et al., 2015). Most of influx transporters (TBDR, ABC) and Zn-free paralogs of Zn proteins were reported to carry putative *Zur* boxes. Under deficiency, this regulator borne by the *ZnuABC* gene cluster facilitates capture of Zn from extracellular medium, while under excess Zn it represses the gene to prevent uptake (Suryawati, 2018) *via* allosteric coupling and alteration of affinity of Zur to DNA binding sites of the Ton B promoter. Thus, Zur plays a cardinal role, highlighting its importance in regulating a plethora of genes involved in Zn homeostasis (Mikhaylina et al., 2018).

Apart from Zur, identification of other regulators like CzcR positively regulating CzcCBA efflux pump, ZntR regulating ZntA, CzcD/ZitB, YiiP, CzcCBA and CusFCBA (Capdevila et al., 2016; Gonzalez et al., 2019) indicated prevalence of a robust regulatory system involved in exporting Zn under excess. ZntR has a femtomolar sensitivity to Zn ions and can bind up to two Zn ions per monomer (Wang et al., 2012)) and presence of both ZntR and Zur implicated an overlap in their sigmoidal activity function to maintain free cytoplasmic Zn within the homeostatic concentration window between 2×10^{-16} M and 10^{-15} M (Outten et al., 1999). CzcRS is a TC system which helps in regulation of export of Zn from cytoplasm to periplasm by regulating cation diffusion facilitator CzcD (Gonzalez et al., 2019). Both *CzcR* as well as *CzcD* have Zur boxes in their upstream regulatory region and could probably be regulated by Zur (Ducret et al., 2023). The co-location of CzcRS TCS on the promoters of virulence factors as well as involvement of CzcR in quorum sensing related virulence of bacteria indicated its role in pathogenicity as well (Gonzalez et al., 2019). Thus, the large set of sensing and signal transduction systems deployed to detect and adapt to excess Zn might be closely related to pathogenesis as many of them are known to control a range of virulence factors (Francis et al., 2017). This is a matter of

concern during nZnO accumulation in soils. Identification of additional transcriptional regulators ArsR/SmtB regulating SmtA indicated either control of Zn occurring at the regulatory interface between Zn import and export by smtB-zur operon or its linkage with Zn exporting P-type ATPases (Riccardi et al., 2008). Abundance of efflux regulator *ZraR*, involved in regulation of ZraP, a chaperone that binds to Zn^{2+} and Cu^{2+} with higher affinity to Cu^{2+} (Van der Weel et al., 2019), indicated a probable cross talk between the two homeostatic pathways. In Zn treatments as nZnO or bZnO, abundance of the periplasmic protein CpxP indicated a negative regulation of the CpxAR system involved in combating envelope stress to re-establish homeostasis (Backstrom et al., 2017). Further, qPCR expression profiling of major resistance genes *CzcA, ZntA* and *YiiP* seamlessly aligned with the metagenomic data (Fig. 4), indicating PMP as an appropriate strategy for such broad scale ecological studies.

5. Conclusion

The bacterial transcriptional regulatory circuits involving Zn varied markedly between Zn deficient and excess treatments and a size-dependent and clearer threshold in gene family abundances were discernible at 1000 mg Zn kg^{-1}. While passive import, energy driven active acquisition, high and low affinity influx as well as Zn sequestration were enhanced under nZnO, primary and secondary detoxifying systems and systems mediating adaptation to anaerobic lifestyle and chelation of Zn were enhanced under bZnO. The dominant genera under nZnO deployed an active shunting strategy for detoxification, while minor uptake systems did not necessitate an active shunting mechanism under bZnO. Moreover, during Zn efflux, dominant genera under nZnO were affiliated with secondary filter proteins, while those under bZnO were mediated by high resistance efflux system. Contribution of genera to the ZHG profile was higher under nZnO, suggesting the possibility of greater recruitment of bacteria for ZHG functions due to a more disturbed environment than bZnO. Zn homeostasis related link with biofilm formation and virulence could pose a potential environmental threat under nZnO toxicity. qRT-PCR analysis of representative resistance genes confirmed that they were modulated by Zn and thus validated the amplicon data. Our study also highlighted the high adaptability of bacterial communities under both Zn scarcity and excess with Zur governing homeostasis in a much more profound manner with moonlighting functions other than uptake and efflux systems and can be considered as the keystone regulator of bacterial Zn homeostasis in nZnO polluted soils. The capabilities of the host taxa contributing towards microbiome stability *viz., Sphingomonas* could be harnessed to remediate nZnO polluted soils. Apparently, in bZnO amended soils, the more tolerant core species played a pivotal role in relieving Zn toxicity and regulating Zn homeostasis by upregulation of Zn detoxifying and tolerant efflux genes. Co-occurrence network indicated the coevality of both influx and efflux genes in majority of the core bacteria which suggested a close nexus between the ZHGs. Overall, the results indicated that higher concentrations of both nZnO and bZnO were hazardous to the soil bacterial communities and at eco-toxicologically relevant concentration, nZnO was more toxic than bZnO. Further studies should involve long-term validation of the nZnO detoxification capabilities of core soil bacterial strains and development of new strategies to remediate nZnO contaminated soils. Needless to say, the machinations involving additional bacterial pathways that minimize and repair nZnO induced damages involving enterobacterial systems responsible for integrity and function of cell envelope, redox balance and detoxification are also worth exploring in such polluted soils.

CRediT authorship contribution statement

Dinesh Raghavan: Conceptualization, Funding acquisition, Methodology, Supervision, Writing – review & editing. **Sreena Chuvatte Patinharekkara**: Investigation, Data curation, Formal analysis, Writing – review & editing. **Sheeja Thotten Elampilay**: Investigation, Methodology, Project administration, Writing – original draft. **Vijesh Kumar Illathidath Payatatti**: Validation. **Sona Charles**: Data curation, Data analysis, Software. **Srinivasan Veeraraghavan**: Resources, Methodology. **Jayarajan Kadiyalath**: Database creation, Statistical analysis. **Sajith Vandana**: Investigation. **Subila Kizhakke Purayil**: Investigation. **Haritha Prasadam**: Investigation. **Shalini Jayaraj Anitha**: Investigation.

Declaration of Competing Interest

The authors declare that they have no known competing financial interests or personal relationships that could have appeared to influence the work reported in this paper.

Data availability

Data will be made available on request.

Acknowledgements

This work was funded by ICAR-National Agricultural Science Fund (ICAR-NASF), New Delhi, India, vide sanction F. No. NASF/GTR-8021/2020–21/220.

Appendix A. Supporting information

Supplementary data associated with this article can be found in the online version at doi:10.1016/j.ecoenv.2023.115222.

References

Ammendola, S., Pasquali, P., Pistoia, C., Petrucci, P., Petrarca, P., Rotilio, G., Battistoni, A., 2007. High-affinity Zn^{2+} uptake system ZnuABC is required for bacterial zinc homeostasis in intracellular environments and contributes to the virulence of *Salmonella enterica*. Infect. Immun. 75, 5867–5876. https://doi.org/10.1128/IAI.00559-07.

Aruoja, V., Dubourguier, H.C., Kasemets, K., Kahru, A., 2009. Toxicity of nanoparticles of CuO, ZnO and TiO_2 to microalgae *Pseudokirchneriella subcapitata*. Sci. Total Environ. 407, 1461–1468. https://doi.org/10.1016/j.scitotenv.2008.10.053.

Assenov, Y., Ramírez, F., Schelhorn, S.-E., Lengauer, T., Albrecht, M., 2008. Computing topological parameters of biological networks. Bioinformatics 24, 282–284. https://doi.org/10.1093/bioinformatics/btm554.

Auti, A.M., Narwade, N.P., Deshpande, N.M., Dhotre, D.P., 2019. Microbiome and imputed metagenome study of crude and refined petroleum-oil-contaminated soils: Potential for hydrocarbon degradation and plant-growth promotion. J. Biosci. 44, 114. https://doi.org/10.1007/s12038-019-9936-9.

Backstrom, I., Johnson, I.H., Lien, S., Ragotte, R., 2017. *cpxP* deletion confers resistance to misfolded PapE induced cytotoxicity through enhanced CpxAR activation in *Escherichia coli*. J. Exp. Microbiol. Immunol. 3, 10–16.

Beard, S.J., Hashim, R., Wu, G., Binet, M.R., Hughes, M.N., Poole, R.K., 2000. Evidence for the transport of zinc (II) ions via the pit inorganic phosphate transport system in *Escherichia coli*. FEMS Microbiol. Lett. 184, 231–235. https://doi.org/10.1111/j.1574-6968.2000.tb09019.x.

Behera, M., Dandapat, J., Rath, C.C., 2014. Effect of heavy metals on growth response and antioxidant defense protection in *Bacillus cereus*. J. Basic Microbiol 54, 1201–1209. https://doi.org/10.1002/jobm.201300805.

Blencowe, D.K., Morby, A.P., 2003. Zn (II) metabolism in prokaryotes. FEMS Microbiol. Rev. 27, 291–311. https://doi.org/10.1016/S0168-6445(03)00041-X.

Blindauer, C.A., 2015. Advances in the molecular understanding of biological zinc transport. Chem. Commun. (Camb.). 51, 4544–4563. https://doi.org/10.1039/c4cc10174j.

Blindauer, C.A., Leszczyszyn, O.I., 2010. Metallothioneins: unparalleled diversity in structures and functions for metal ion homeostasis and more. Nat. Prod. Rep. 27, 720–741. https://doi.org/10.1039/b906685n.

Bobrov, A.G., Kirillina, O., Fetherston, J.D., Miller, M.C., Burlison, J.A., Perry, R.D., 2014. The *Yersinia pestis* siderophore, yersiniabactin, and the ZnuABC system both contribute to zinc acquisition and the development of lethal septicaemic plague in mice. Mol. Microbiol. 93, 759–775. https://doi.org/10.1111/mmi.12693.

Botella, H., Peyron, P., Levillain, F., Poincloux, R., Poquet, Y., Brandli, I., Wang, C., Tailleux, L., Tilleul, S., Charrière, G.M., Waddell, S.J., Foti, M., Lugo-Villarino, G., Gao, Q., Maridonneau-Parini, I., Butcher, P.D., Castagnoli, P.R., Gicquel, B., de Chastellier, C., Neyrolles, O., 2011. Mycobacterial p (1)-type ATPases mediate resistance to zinc poisoning in human macrophages. Cell Host Microbe 10, 248–259. https://doi.org/10.1016/j.chom.2011.08.006.

Capdevila, D.A., Wang, J., Giedroc, D.P., 2016. Bacterial strategies to maintain zinc metallostasis at the host-pathogen interface. J. Biol. Chem. 291, 20858–20868. https://doi.org/10.1074/jbc.R116.742023.

Chandrangsu, P., Helmann, J.D., 2016. Intracellular Zn (II) intoxication leads to dysregulation of the PerR regulon resulting in heme toxicity in *Bacillus subtilis*. PLoS Genet 12, e1006515. https://doi.org/10.1371/journal.pgen.1006515.

Chaoprasid, P., Nookabkaew, S., Sukchawalit, R., Mongkolsuk, S., 2015. Roles of *Agrobacterium tumefaciens* C58 ZntA and ZntB and the transcriptional regulator ZntR in controlling $Cd^{2+}/Zn^{2+}/Co^{2+}$ resistance and the peroxide stress response. Microbiology 161, 1730–1740. https://doi.org/10.1099/mic.0.000135.

Chen, C., Unrine, J.M., Hu, Y., Guo, L., Tsyusko, O.V., Fan, Z., Liu, S., Wei, G., 2021. Responses of soil bacteria and fungal communities to pristine and sulfidized zinc oxide nanoparticles relative to Zn ions. J. Hazard. Mater. 405, 124258 https://doi.org/10.1016/j.jhazmat.2020.124258.

Compan, I., Touati, D., 1994. Anaerobic activation of arcA transcription in *Escherichia coli*: roles of Fnr and ArcA. Mol. Microbiol. 11, 955–964. https://doi.org/10.1111/j.1365-2958.1994.tb00374.x.

Dinesh, R., Sreena, C.P., Sheeja, T.E., Charles, S., Srinivasan, V., Sajith, V., Subila, K.P., Haritha, P., 2023a. Metagenomics indicates abundance of biofilm related genes and horizontal transfer of multidrug resistant genes among bacterial communities in nano zinc oxide polluted soil. Sci. Total Environ. 859, 160032 https://doi.org/10.1016/j.scitotenv.2022.160032.

Dinesh, R., Sreena, C.P., Sheeja, T.E., Kumar, I.P.V., Praveena, R., Charles, S., Srinivasan, V., Jayarajan, K., Sajith, V., Subila, K.P., Haritha, P., 2023b. Soil polluted with nano ZnO reveals unstable bacterial communities and decoupling of taxonomic and functional diversities. Sci. Total Environ. 889, 164285 https://doi.org/10.1016/j.scitotenv.2023.164285.

Ducret, V., Abdou, M., GoncalvesMilho, C., Leoni, S., Martin-Pelaud, O., Sandoz, A., Segovia Campos, I., Tercier-Waeber, M.-L., Valentini, M., Perron, K., 2021. Global analysis of the zinc homeostasis network in *Pseudomonas aeruginosa* and its gene expression dynamics. Front. Microbiol. 12, 739988 https://doi.org/10.3389/fmicb.2021.739988.

Ducret, V., Gonzalez, D., Perron, K., 2022. Zinc homeostasis in *Pseudomonas*. Biometals 1–16. https://doi.org/10.1007/s10534-022-00475-5.

Ducret, V., Gonzalez, D., Leoni, S., Valentini, M., Perron, K., 2023. A Zur-mediated transcriptional regulation of the zinc export system in *Pseudomonas aeruginosa*. BMC Microbiol 23, 6. https://doi.org/10.1186/s12866-022-02750-4.

Eixenberger, J.E., Anders, C.B., Hermann, R.J., Brown, R.J., Reddy, K.M., Punnoose, A., Wingett, D.G., 2017. Rapid dissolution of ZnO nanoparticles induced by biological buffers significantly impacts cytotoxicity. Chem. Res. Toxicol. 30, 1641–1651. https://doi.org/10.1021/acs.chemrestox.7b00136.

Francis, V.I., Stevenson, E.C., Porter, S.L., 2017. Two-component systems required for virulence in *Pseudomonas aeruginosa*. FEMS Microbiol. Lett. 364. https://doi.org/10.1093/femsle/fnx104.

Gati, C., Stetsenko, A., Slotboom, D.J., Scheres, S.H.W., Guskov, A., 2017. The structural basis of proton driven zinc transport by ZntB. Nat. Commun. 8, 1313. https://doi.org/10.1038/s41467-017-01483-7.

Ghosh, M., Jana, A., Sinha, S., Jothiramajayam, M., Nag, A., Chakraborty, A., Mukherjee, Amitava, Mukherjee, Anita, 2016. Effects of ZnO nanoparticles in plants: Cytotoxicity, genotoxicity, deregulation of antioxidant defenses, and cell-cycle arrest. Mutat. Res. Genet. Toxicol. Environ. Mutagen. 807, 25–32. https://doi.org/10.1016/j.mrgentox.2016.07.006.

Gillan, D.C., 2016. Metal resistance systems in cultivated bacteria: are they found in complex communities? Curr. Opin. Biotechnol. 38, 123–130. https://doi.org/10.1016/j.copbio.2016.01.012.

Gonzalez, M.R., Ducret, V., Leoni, S., Perron, K., 2019. *Pseudomonas aeruginosa* zinc homeostasis: Key issues for an opportunistic pathogen. Biochim. Biophys. Acta Gene Regul. Mech. 1862, 722–733. https://doi.org/10.1016/j.bbagrm.2018.01.018.

Grass, G., Fan, B., Rosen, B.P., Franke, S., Nies, D.H., Rensing, C., 2001. ZitB (YbgR), a member of the cation diffusion facilitator family, is an additional zinc transporter in *Escherichia coli*. J. Bacteriol. 183, 4664–4667. https://doi.org/10.1128/JB.183.15.4664-4667.2001.

Grass, G., Franke, S., Taudte, N., Nies, D.H., Kucharski, L.M., Maguire, M.E., Rensing, C., 2005. The metal permease ZupT from *Escherichia coli* is a transporter with a broad substrate spectrum. J. Bacteriol. 187, 1604–1611. https://doi.org/10.1128/JB.187.5.1604-1611.2005.

Hantke, K., 2001. Bacterial zinc transporters and regulators. Biometals 14, 239–249. https://doi.org/10.1023/a:1012984713391.

Hantke, K., 2005. Bacterial zinc uptake and regulators. Curr. Opin. Microbiol. 8, 196–202. https://doi.org/10.1016/j.mib.2005.02.001.

Heinlaan, M., Ivask, A., Blinova, I., Dubourguier, H.-C., Kahru, A., 2008. Toxicity of nanosized and bulk ZnO, CuO and TiO_2 to bacteria *Vibrio fischeri* and crustaceans *Daphnia magna* and *Thamnocephalus platyurus*. Chemosphere 71, 1308–1316. https://doi.org/10.1016/j.chemosphere.2007.11.047.

Hu, X., Wang, J., Lv, Y., Liu, X., Zhong, J., Cui, X., Zhang, M., Ma, D., Yan, X., Zhu, X., 2021. Effects of heavy metals/metalloids and soil properties on microbial communities in farmland in the vicinity of a metal smelter. Front. Microbiol. 12, 707786 https://doi.org/10.3389/fmicb.2021.707786.

Hund-Rinke, K., Schlich, K., Klawonn, T., 2012. Influence of application techniques on the ecotoxicological effects of nanomaterials in soil. Environ. Sci. Eur. 24, 30. https://doi.org/10.1186/2190-4715-24-30.

Jani, K., Ghattargi, V., Pawar, S., Inamdar, M., Shouche, Y., Sharma, A., 2018. Anthropogenic activities induce depletion in microbial communities at urban sites of the river ganges. Curr. Microbiol. 75, 79–83. https://doi.org/10.1007/s00284-017-1352-5.

Jubelin, G., Vianney, A., Beloin, C., Ghigo, J.-M., Lazzaroni, J.-C., Lejeune, P., Dorel, C., 2005. CpxR/OmpR interplay regulates curli gene expression in response to osmolarity in *Escherichia coli*. J. Bacteriol. 187, 2038–2049. https://doi.org/10.1128/JB.187.6.2038-2049.2005.

Kandari, D., Gopalani, M., Gupta, M., Joshi, H., Bhatnagar, S., Bhatnagar, R., 2019. Identification, Functional characterization, and regulon prediction of the zinc uptake regulator (zur) of *Bacillus anthracis* - An insight into the zinc homeostasis of the pathogen. Front. Microbiol. 9, 3314. https://doi.org/10.3389/fmicb.2018.03314.

Lindsay, W.L., Norvell, W.A., 1978. Development of a DTPA soil test for Zn, iron, manganese, and copper. Soil Sci. Soc. Am. J. 42, 421–428. https://doi.org/10.2136/sssaj1978.03615995004200030009x.

Lu, M., Fu, D., 2007. Structure of the zinc transporter YiiP. Science 317, 1746–1748. https://doi.org/10.1126/science.1143748.

Meli, K., Kamika, I., Keshri, J., Momba, M.N.B., 2016. The impact of zinc oxide nanoparticles on the bacterial microbiome of activated sludge systems. Sci. Rep. 6, 39176. https://doi.org/10.1038/srep39176.

Mikhaylina, A., Ksibe, A.Z., Scanlan, D.J., Blindauer, C.A., 2018. Bacterial zinc uptake regulator proteins and their regulons. Biochem. Soc. Trans. 46, 983–1001. https://doi.org/10.1042/BST20170228.

Moore, C.M., Helmann, J.D., 2005. Metal ion homeostasis in *Bacillus subtilis*. Curr. Opin. Microbiol. 8, 188–195. https://doi.org/10.1016/j.mib.2005.02.007.

Nies, D.H., 2003. Efflux-mediated heavy metal resistance in prokaryotes. FEMS Microbiol. Rev. 27, 313–339. https://doi.org/10.1016/S0168-6445(03)00048-2.

Nongkhlaw, M., Joshi, S.R., 2019. Molecular insight into the expression of metal transporter genes in *Chryseobacterium* sp. PMSZPI isolated from uranium deposit. PLoS One 14, e0216995. https://doi.org/10.1371/journal.pone.0216995.

Outten, C.E., Outten, F.W., O'Halloran, T.V., 1999. DNA distortion mechanism for transcriptional activation by ZntR, a Zn (II)-responsive MerR homologue in *Escherichia coli*. J. Biol. Chem. 274, 37517–37524. https://doi.org/10.1074/jbc.274.53.37517.

Ouyang, A., Gasner, K.M., Neville, S.L., McDevitt, C.A., Frawley, E.R., 2022. MntP and YiiP contribute to manganese efflux in *Salmonella enterica* Serovar *typhimurium* under conditions of manganese overload and nitrosative stress. Microbiol. Spectr. 10, e0131621 https://doi.org/10.1128/spectrum.01316-21.

Pederick, V.G., Eijkelkamp, B.A., Begg, S.L., Ween, M.P., McAllister, L.J., Paton, J.C., McDevitt, C.A., 2015. ZnuA and zinc homeostasis in *Pseudomonas aeruginosa*. Sci. Rep. 5, 13139. https://doi.org/10.1038/srep13139.

Peng, Y.-H., Tsai, Y.-C., Hsiung, C.-E., Lin, Y.-H., Shih, Y.-H., 2017. Influence of water chemistry on the environmental behaviors of commercial ZnO nanoparticles in various water and wastewater samples. J. Hazard. Mater. 322, 348–356. https://doi.org/10.1016/j.jhazmat.2016.10.003.

Petit-Härtlein, I., Rome, K., de Rosny, E., Molton, F., Duboc, C., Gueguen, E., Rodrigue, A., Covès, J., 2015. Biophysical and physiological characterization of ZraP from *Escherichia coli*, the periplasmic accessory protein of the atypical ZraSR two-component system. Biochem. J. 472, 205–216. https://doi.org/10.1042/BJ20150827.

Riccardi, G., Milano, A., Pasca, M.R., Nies, D.H., 2008. Genomic analysis of zinc homeostasis in *Mycobacterium tuberculosis*. FEMS Microbiol. Lett. 287, 1–7. https://doi.org/10.1111/j.1574-6968.2008.01320.x.

Sabri, M., Caza, M., Proulx, J., Lymberopoulos, M.H., Brée, A., Moulin-Schouleur, M., Curtiss, R., Dozois, C.M., 2008. Contribution of the SitABCD, MntH, and FeoB metal transporters to the virulence of avian pathogenic *Escherichia coli* O78 strain chi7122. Infect. Immun. 76, 601–611. https://doi.org/10.1128/IAI.00789-07.

Sabri, M., Houle, S., Dozois, C.M., 2009. Roles of the extraintestinal pathogenic *Escherichia coli* ZnuACB and ZupT zinc transporters during urinary tract infection. Infect. Immun. 77, 1155–1164. https://doi.org/10.1128/IAI.01082-08.

Salam, L.B., Obayori, O.S., Ilori, M.O., Amund, O.O., 2020. Effects of cadmium perturbation on the microbial community structure and heavy metal resistome of a tropical agricultural soil. Bioresour. Bioprocess. 7, 25. https://doi.org/10.1186/s40643-020-00314-w.

Shannon, P., Markiel, A., Ozier, O., Baliga, N.S., Wang, J.T., Ramage, D., Amin, N., Schwikowski, B., Ideker, T., 2003. Cytoscape: a software environment for integrated models of biomolecular interaction networks. Genome Res 13, 2498–2504. https://doi.org/10.1101/gr.1239303.

Shen, Q., Tang, J., Wang, X., Li, Y., Yao, X., Sun, H., Wu, Y., 2021. Fate of antibiotic resistance genes and metal resistance genes during the thermophilic fermentation of solid and liquid swine manures in an ectopic fermentation system. Ecotoxicol. Environ. Saf. 213, 111981 https://doi.org/10.1016/j.ecoenv.2021.111981.

Shen, Z., Chen, Z., Hou, Z., Li, T., Lu, X., 2015. Ecotoxicological effect of zinc oxide nanoparticles on soil microorganisms. Front. Environ. Sci. Eng. 9, 912–918. https://doi.org/10.1007/s11783-015-0789-7.

Singh, R., Cheng, S., Singh, S., 2020. Oxidative stress-mediated genotoxic effect of zinc oxide nanoparticles on *Deinococcus radiodurans*. 3 Biotech 10, 66. https://doi.org/10.1007/s13205-020-2054-4.

Suryawati, B., 2018. Zinc homeostasis mechanism and its role in bacterial virulence capacity. AIP Conf. Proc. 2021, 070021 https://doi.org/10.1063/1.5062819.

Van der Weel, L., As, K.S., Dekker, W.J.C., van den Eijnden, L., van Helmond, W., Schiphorst, C., Hagen, W.R., Hagedoorn, P.-L., 2019. ZraP, the most prominent zinc protein under zinc stress conditions has no direct role in *in vivo* zinc tolerance in *Escherichia coli*. J. Inorg. Biochem. 192, 98–106. https://doi.org/10.1016/j.jinorgbio.2018.12.013.

Wang, D., Hosteen, O., Fierke, C.A., 2012. ZntR-mediated transcription of zntA responds to nanomolar intracellular free zinc. J. Inorg. Biochem. 111, 173–181. https://doi.org/10.1016/j.jinorgbio.2012.02.008.

Wątły, J., Potocki, S., Rowińska-Żyrek, M., 2016. Zinc homeostasis at the bacteria/host interface-from coordination chemistry to nutritional immunity. Chemistry 22, 15992–16010. https://doi.org/10.1002/chem.201602376.

Xia, P., Lian, S., Wu, Y., Yan, L., Quan, G., Zhu, G., 2021. Zinc is an important inter-kingdom signal between the host and microbe. Vet. Res. 52, 39. https://doi.org/10.1186/s13567-021-00913-1.

Xiao, M., Lai, Y., Sun, J., Chen, G., Yan, A., 2016. Transcriptional regulation of the outer membrane porin gene ompW reveals its physiological role during the transition from the aerobic to the anaerobic lifestyle of *Escherichia coli*. Front. Microbiol. 7, 799. https://doi.org/10.3389/fmicb.2016.00799.

Xu, X., Guo, H., Wang, X., Zhang, M., Wang, Z., Yang, B., 2019. Physical properties and anti-aging characteristics of asphalt modified with nano-zinc oxide powder. Constr. Build. Mater. 224, 732–742. https://doi.org/10.1016/j.conbuildmat.2019.07.097.

Zhao, L., Peralta-Videa, J.R., Ren, M., Varela-Ramirez, A., Li, C., Hernandez-Viezcas, J. A., Aguilera, R.J., Gardea-Torresdey, J.L., 2012. Transport of Zn in a sandy loam soil treated with ZnO NPs and uptake by corn plants: electron microprobe and confocal microscopy studies. Chem. Eng. J. 184, 1–8. https://doi.org/10.1016/j.cej.2012.01.04.

Zhao, Q., Guo, W., Luo, H., Xing, C., Wang, H., Liu, B., Si, Q., Ren, N., 2021. Deciphering the transfers of antibiotic resistance genes under antibiotic exposure conditions: Driven by functional modules and bacterial community. Water Res 205, 117672. https://doi.org/10.1016/j.watres.2021.117672.